

Large curvature perturbations near horizon crossing in single-field inflation models

Edgar Bugaev and Peter Klimai*

Institute for Nuclear Research, Russian Academy of Sciences,
60th October Anniversary Prospect 7a, 117312 Moscow, Russia

Abstract

We consider the examples of single-field inflation models predicting large amplitudes of the curvature perturbation power spectrum at relatively small scales. It is shown that in models with an inflationary potential of double-well type the peaks in the power spectrum, having, in maximum, the amplitude $\mathcal{P}_{\mathcal{R}} \sim 0.1$, can exist (if parameters of the potential are chosen appropriately). It is shown also that the spectrum amplitude of the same magnitude (at large k values) is predicted in the model with the running mass potential, if the positive running, n' , exists and is about 0.005.

1 Introduction

In last few months several papers appeared [1, 2, 3, 4], in which single-field inflation models predicting (potentially) large amplitudes of the curvature perturbations on relatively small scales are discussed. It is shown in [1] that large class of such models exists, namely, the models with a potential of hill-top type (the idea of the hill-top inflation was proposed, to author's knowledge, in the earlier work [5]). In such models, the potential can be of concave-downward form at cosmological scales (in accordance with data) and be much flatter at the end of inflation when small scales leave horizon. Correspondingly, the amplitude of the perturbation power spectrum can be rather large. It is noticed in [1] that the running mass model, having the potential with the similar behavior, also can predict the large spectrum amplitude.

Authors of [2] discuss also more general scenarios of producing large amplitudes of perturbation spectrum. They show the limitedness of the standard procedure of the potential reconstruction which can easily miss the potentials leading to large spectrum amplitude and even to primordial black hole (PBH) production.

In the recent paper [3] it was shown that PBH production is possible in single-field models of two-stage type ("chaotic + new"). The idea was proposed ten years ago in [6]. Authors of [3] carried out the numerical calculation of the power spectrum using the Coleman-Weinberg (CW) potential.

In the present paper we continue the study of the problems discussed in previous works [1, 2, 3]. We investigated thoroughly, as a particular example, the model of two-stage inflation with a potential of the double-well (DW) form, and showed that the characteristic features of the power spectrum in models of this type (such as an amplitude and a position of the peak, a degree of tuning of parameters of the potential) are very sensitive to an exact form of the

*e-mail: pklimai@gmail.com

potential. Further, we carried out the numerical calculation of the power spectrum in running mass model and showed that the spectrum amplitude at small scales can be rather large. Our calculation differs from the previous one [7] in several aspects: we express the results through the values of parameters s , c , which are used nowadays and prove to be very convenient for a comparison with data; we studied, in details, the difference in predictions of slow-roll and numerical approaches at high k -values; we exactly specified the value of the positive running, n' , which corresponds to our spectrum prediction. In the final part of the work we investigated the quantum diffusion effects in a model with the running mass potential.

The plan of the paper is as follows. At the end of this introduction we give, for completeness, the main formulae required for a calculation of the curvature perturbation power spectrum, both in the slow-roll approximation and in the numerical approach. In the next section we study predictions of two-stage inflation models with DW and CW potentials, with accent on a mechanism of the formation of peaks in the power spectrum. In the Sec. 3 all aspects connected with an obtaining of the predictions of running mass inflation models are discussed. In Sec. 4 we present our main conclusions.

Primordial density perturbation can be expressed in terms of the intrinsic curvature perturbation on comoving hypersurfaces \mathcal{R} [8], given by

$$\mathcal{R} = R - \frac{H}{\dot{\phi}} \delta\phi \quad (1)$$

during inflation, where ϕ is the inflaton field, R is the scalar describing the spatial curvature in the perturbed line element around a FLRW universe, and dot denotes the derivative over cosmic time t . The standard result for the power spectrum of the curvature perturbation to leading order in the slow-roll approximation is [9, 10, 11, 12]

$$\mathcal{P}_{\mathcal{R}}(k) = \frac{H^2}{\pi \epsilon m_{Pl}^2} \Big|_{aH=k}, \quad (2)$$

and to first order is [13]

$$\mathcal{P}_{\mathcal{R}}^{1/2}(k) = [1 - (2C + 1)\epsilon + C\eta] \frac{1}{2\pi} \frac{H^2}{|\dot{\phi}|} \Big|_{aH=k}; \quad C \approx -0.73. \quad (3)$$

In these expressions we use the usual notations for the slow-roll parameters,

$$\epsilon = -\frac{\dot{H}}{H^2} = \frac{4\pi}{m_{Pl}^2} \frac{\dot{\phi}^2}{H^2}, \quad \eta = -\frac{\ddot{\phi}}{H\dot{\phi}}. \quad (4)$$

Recently, the power spectrum and spectral index were calculated with taking into account second order corrections [14].

For an accurate numerical calculation of the power spectrum, it is quite convenient to use the formalism of gauge invariant cosmological perturbation theory [8, 9, 10]. The curvature perturbation \mathcal{R} can be written using the new variable u [8, 9, 10],

$$\mathcal{R} = \frac{u}{z}, \quad u \equiv a \left(\delta\phi - \frac{\dot{\phi}}{H} R \right), \quad z \equiv \frac{a\dot{\phi}}{H}. \quad (5)$$

It follows from eq. (5) that in the spatially flat gauge (where $R = 0$) one has

$$u = a\delta\phi, \quad \mathcal{R} = H \frac{\delta\phi}{\dot{\phi}}. \quad (6)$$

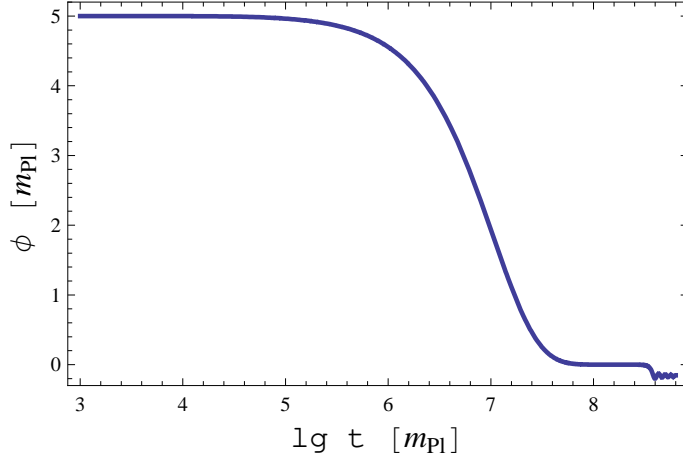


Figure 1: The solution of the background equation for inflation with the double-well potential (13). The parameters of the potential are: $v = 0.16286748 m_{Pl}$, $\lambda = 1.7 \times 10^{-13}$.

The physical sense of the variable u is clear from eq. (6): u/a is the inflaton field perturbation in the spatially flat gauge. The curvature perturbation, as a function of the conformal time τ , is the solution of the differential equation (prime denotes the derivative over τ)

$$\mathcal{R}_k'' + 2\frac{z'}{z}\mathcal{R}_k' + k^2\mathcal{R}_k = 0, \quad (7)$$

$$\frac{z'}{z} = aH(1 + \epsilon - \eta). \quad (8)$$

Here, \mathcal{R}_k is the Fourier component of \mathcal{R} ,

$$\mathcal{R}_k(\tau) = \frac{1}{(2\pi)^3} \int e^{-i\vec{k}\vec{x}} \mathcal{R}(\vec{x}, \tau) d^3x. \quad (9)$$

The power spectrum of scalar curvature perturbations is given by

$$\mathcal{P}_{\mathcal{R}}(k) = \frac{4\pi k^3}{(2\pi)^3} |\mathcal{R}_k|^2. \quad (10)$$

Sometimes it is more convenient to use the usual time t instead of τ . In this case, equation for \mathcal{R}_k is

$$\ddot{\mathcal{R}}_k + H\dot{\mathcal{R}}_k(3 + 2\epsilon - 2\eta) + \frac{k^2}{a^2}\mathcal{R}_k = 0. \quad (11)$$

The standard initial condition, corresponding to the Bunch-Davies vacuum, is

$$u_k(\tau) = \frac{1}{\sqrt{2k}} e^{-ik\tau}, \quad aH \ll k. \quad (12)$$

Note, that the functions ϵ , η entering the eq. (8) are not necessarily small, in contrast with the case of eqs. (2, 3), where they are slow-roll parameters and where, by definition, $\epsilon \ll 1$, $|\eta| \ll 1$.

2 Examples of the power spectrum with peaks

2.1 Double-well potential

This form of the inflaton potential having an unstable local maximum at the origin has been discussed many times in studies of eternal and new inflation. The main problem was to realize

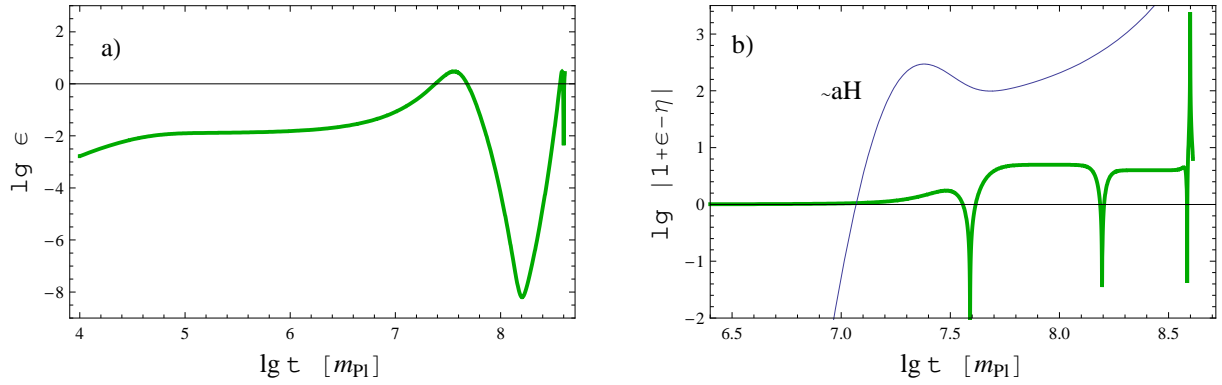


Figure 2: The time dependence of the parameter ϵ and the combination $1 + \epsilon - \eta$ corresponding to the background field evolution shown in fig. 1

the initial condition for the new inflation when system starts from a top of the hill. Ten years ago the model of "chaotic new inflation" has been proposed [6], in which the system climbs on the top during dynamical evolution of the inflaton field with initial conditions coinciding with those of chaotic inflation models. In the approach of [6] the inflation has two stages, chaotic and new, and during transition from the first stage to the second the slow-roll conditions break down (in general).

The potential has two parameters:

$$V(\phi) = \frac{\lambda}{4}(\phi^2 - v^2)^2. \quad (13)$$

The inflaton starts with the rather high value of ϕ (we take $\phi_{\text{in}} \sim 5m_{Pl}$) and rolls down to the origin. The parameter λ is fixed by normalization of the power spectrum on experimental data, $\lambda \sim 10^{-13}$. The evolution of the system strongly depends on the value of v : if v is finely tuned, ϕ can spend some time near the origin, i.e. on the top, and then roll down to one of the two minima. In figs. 1 and 2a the time evolution for the inflaton and parameter ϵ for the definite values of the parameters λ , v are shown. One can see that, really, $\phi \approx 0$ at some period of time and, what is important, the slow-roll approximation is invalid ($\epsilon \sim 1$) just at the time of the transition from a rolling to a temporary stay at the top of the potential.

It is well known that in situations when there is a failure of the slow-roll evolution the perturbations on super-horizon scales can be amplified and specific features in the power spectrum can arise [15, 16, 17, 18]. It means that the predictions of the slow-roll approximation which assumes that perturbations reach an asymptotic regime outside the horizon cannot be trusted.

It had been demonstrated in [17] that the solution of equation for \mathcal{R} at $k \ll aH$, i.e., outside horizon, is well approximated by constant if the coefficient of the friction term, z'/z , doesn't change sign near the horizon crossing. In the opposite case, if z'/z changes sign at some time, the friction term becomes a negative driving term, and one can expect strong effects on modes which left horizon near that time. In the present paper we study the corresponding features of the power spectrum, following closely the analysis of [17].

According to eq. (8), z'/z is proportional to $1 + \epsilon - \eta$ and the comoving Hubble wave number aH . The time dependence of these functions is shown in fig. 2b. One can see that the interruption of inflation correlates with the change of the sign of $1 + \epsilon - \eta$.

The time evolution of curvature perturbations for several modes is shown in fig. 3. It is clearly seen that the perturbations \mathcal{R}_k for different modes freeze out at different amplitudes. The mode which crosses horizon near the moment of time when the sign of $1 + \epsilon - \eta$ changes (i.e., near $t \approx 7.5m_{Pl}$) freezes at maximum amplitude, due to the exponentially growing driving term in eq. (7) (which is most effective just for this mode). It leads to the characteristic peak in the power spectrum shown in fig. 4.

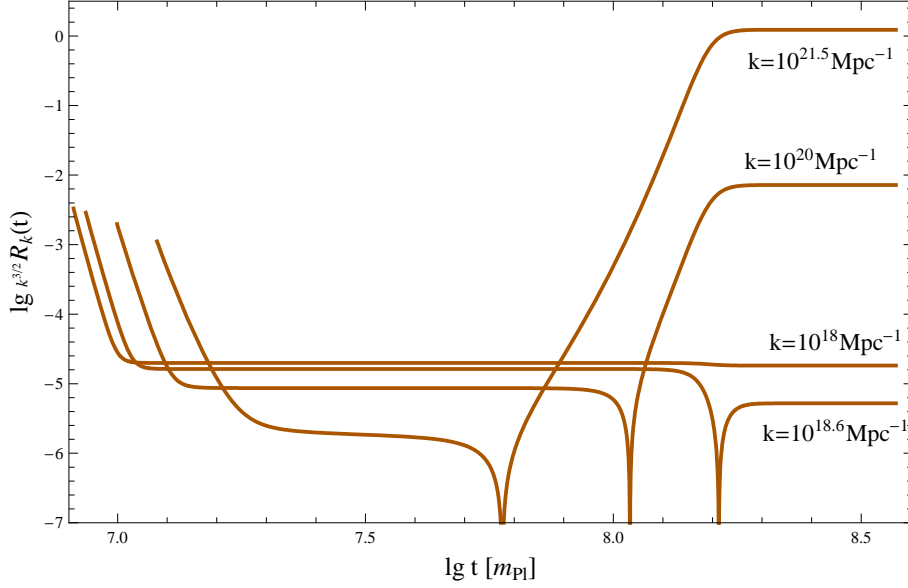


Figure 3: A time evolution of the curvature perturbation $\mathcal{R}_k(t)$ for several different values of wave number k during inflation with the DW potential. The parameters of the potential are the same as in fig. 1.

The calculations of \mathcal{R}_k (fig. 3) are carried out up to the end of inflation, and the power spectrum at fig. 4 also corresponds to this moment of time. We estimate approximately the reheate temperature in our case as $\sim (\lambda v^4)^{1/4} \sim 10^{14}$ GeV. The horizon mass at the beginning of radiation era is

$$M_{hi} \sim 10^{17} \text{g} \left(\frac{10^7 \text{GeV}}{T_{\text{RH}}} \right)^2 \sim 10^3 \text{g}, \quad (14)$$

and maximum wave number, which equals the Hubble radius at the end of inflation, is

$$k_{\text{end}} = a_{\text{eq}} H_{\text{eq}} \left(\frac{M_{\text{eq}}}{M_{hi}} \right)^{1/2} \sim 10^{23} \text{ Mpc}^{-1}. \quad (15)$$

In the fig. 5 we show the power spectrum calculated for two stages of its evolution: at horizon exit (HE) and at the end of inflation (END). In the same figure the result of the calculation with an use of the slow-roll formulae is also shown. The peak of HE curve at the region of large k is due to a failure (for \mathcal{R}_k) to reach the asymptotic limit. One can see also that the slow-roll approximation is too crude to describe perturbations at the end of inflation (this our conclusion agrees with those of [17]).

2.2 Coleman-Weinberg potential

The Coleman-Weinberg potential has the form [6, 19]:

$$V(\phi) = \frac{\lambda}{4} \phi^4 \left(\ln \left| \frac{\phi}{v} \right| - \frac{1}{4} \right) + \frac{\lambda}{16} v^4. \quad (16)$$

It looks very similar to the previous one, but the important difference is its behavior near the origin. Namely, CW potential behaves as $A + B\phi^4 \ln(\phi/v)$ near the origin, i.e., it is more flat near zero, in comparison with DW potential. Therefore, it has more e-folds of "new inflation" and, as a consequence, the peaks of the power spectrum (arising, as in the previous case, due to the temporary interruption of inflation) correspond to relatively smaller k values. In fig. 6 two examples of the power spectrum calculations are shown for two different sets of parameter values. As before, the peaks are very distinct, although their amplitudes are smaller.

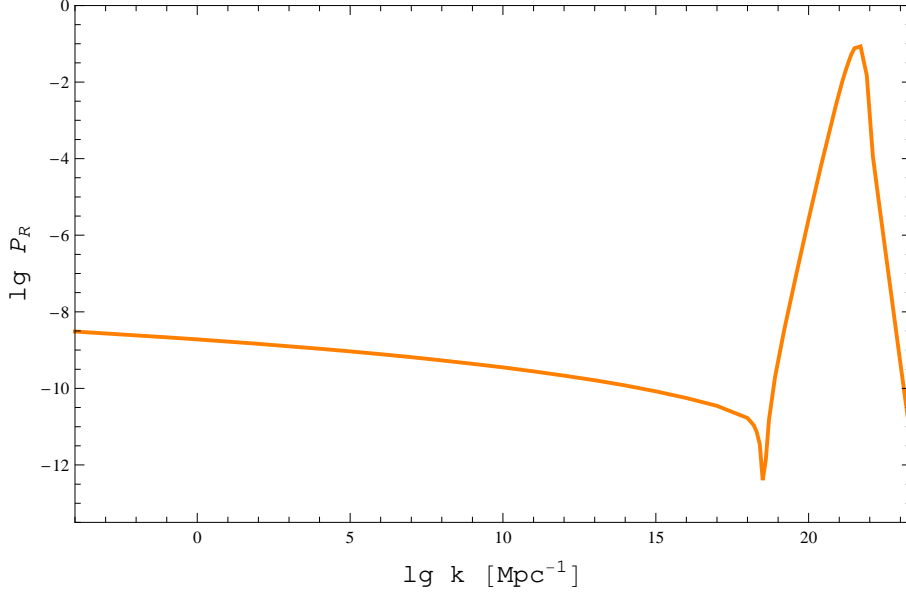


Figure 4: The numerically calculated power spectrum $\mathcal{P}_{\mathcal{R}}(k)$ for the model with the potential (13). Parameters of the potential used in the calculation are the same as in fig. 1.

2.3 Possibilities of PBH production

One can see, in particular, from fig. 4, that, in principle, the production of primordial black holes (about these objects, see original works [20, 21] and reviews [22, 23]) can be rather large in single-field inflation models with potentials of double-well type. The main conclusion is that it requires rather large fine tuning of parameters of the potential. The characteristic PBH mass is estimated by

$$M_{\text{BH}} \approx M_h = M_{hi} \left(\frac{k_{\text{end}}}{k_{\text{peak}}} \right)^2, \quad (17)$$

and in the case of the spectrum of fig. 4, $M_{\text{BH}} \sim 10^7 g$. In the CW case, fig. 6, $M_{\text{BH}} \sim 100 M_{\odot}$ for the left peak and $M_{\text{BH}} \sim 10^{27} g$ for the right peak (but the amplitudes of the spectra are too small).

Recently, it has been shown [3] that inflation with CW potential is capable to produce significant number of PBHs: the parameter v can be chosen (by finest tuning!) in such a way that inflaton field makes several oscillations from one minimum to another before it climbs on the top and "new inflation" starts.

3 Running mass model

3.1 Main assumptions and approximations

We consider in more detail the case of running mass inflation model [24, 25, 26, 27, 28, 29, 30] which predicts a spectral index with rather strong scale dependence. The potential in this case takes into account quantum corrections in the context of softly broken global supersymmetry and is given by the formula

$$V = V_0 + \frac{1}{2} m^2 (\ln \phi) \phi^2. \quad (18)$$

The dependence of the inflaton mass on the renormalization scale ϕ is determined by the solution of the renormalization group equation (RGE).

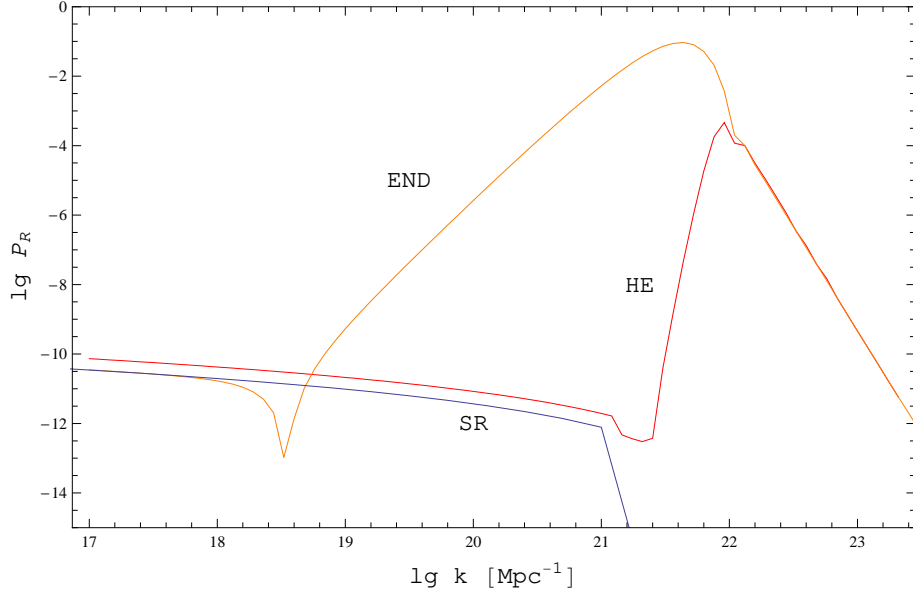


Figure 5: The power spectrum $\mathcal{P}_{\mathcal{R}}(k)$ for the model with potential (13). END: $\mathcal{P}_{\mathcal{R}}(k)$ is calculated at the end of inflation; HE: $\mathcal{P}_{\mathcal{R}}(k)$ is calculated at the time of the horizon exit; SR: the slow-roll result.

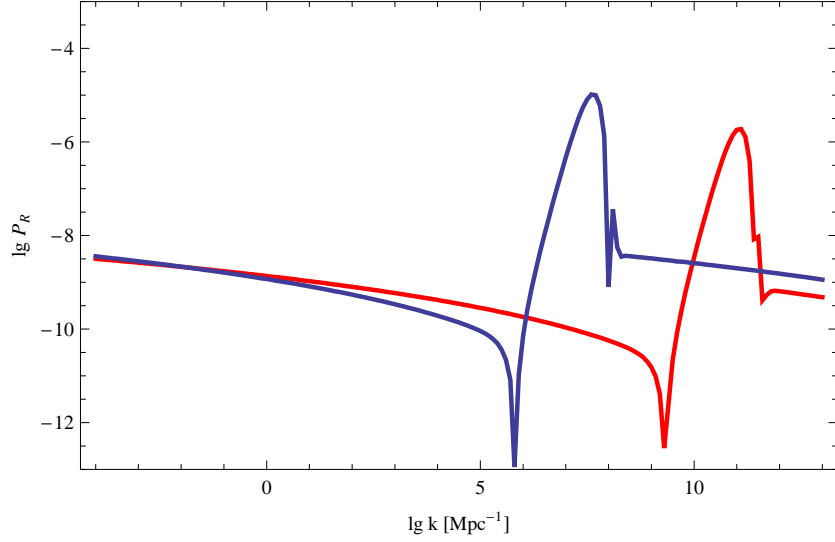


Figure 6: The result for the power spectrum $\mathcal{P}_{\mathcal{R}}(k)$ calculation for the CW potential (16), for two sets of parameters. Left peak is for $v = 1.113M_P$, $\lambda = 5.5 \times 10^{-13}$. For the right peak, $v = 1.112M_P$, $\lambda = 2.4 \times 10^{-13}$.

1. The inflationary potential in supergravity theory is of the order of M_{inf}^4 , where M_{inf} is the scale of supersymmetry breaking during inflation. In turn, the mass-squared of the inflaton (and any other scalar field) in supergravity has, in general, the order of the square of Hubble expansion rate during inflation,

$$|m^2| \sim H_I^2 = \frac{V_0}{3M_P^2}. \quad (19)$$

We suppose, for simplicity (see [24, 25, 27, 28]), that $M_{\text{inf}} \sim M_s$, where M_s is the scale of supersymmetry breaking in the vacuum,

$$M_s \sim \sqrt{\tilde{m}_s M_P} \sim 10^{11} \text{ GeV} \sim 3 \times 10^{-8} M_P \quad (20)$$

(\tilde{m}_s is the scale of squarks and slepton masses, $\tilde{m}_s \sim 3 \text{ TeV}$). These assumptions give the scale of the inflationary potential:

$$V_0 \sim M_s^4 \sim 10^{-30} M_P^4, \quad H_I \approx 10^{-15} M_P. \quad (21)$$

2. RGE for the inflaton mass is the following (we consider a model [27, 28] of hybrid inflation using the softly broken SUSY with gauge group $SU(N)$ and small Yukawa coupling):

$$m^2(t) = m_0^2 - A\tilde{m}_0^2 \left[1 - \frac{1}{(1 + \tilde{\alpha}_0 t)^2} \right], \quad t \equiv \ln \frac{\phi}{M_P}, \quad (22)$$

m_0^2 and \tilde{m}_0^2 are, correspondingly, the inflaton and gaugino masses at $\phi = M_P$,

$$\tilde{\alpha}_0 = \frac{B\alpha_0}{2\pi}, \quad (23)$$

α_0 is the gauge coupling constant, $\alpha_0 = g^2/4\pi$. A and B are positive numbers of order 1, which are different for different variants of the model, even if they are based on the same supersymmetric gauge group $SU(N)$ (it depends on a form of the superpotential, particle content of supermultiplets, etc). We use in the present paper the variant of [28] and, correspondingly, put everywhere below $A = 2$ and $B = N = 2$.

3. A truncated Taylor expansion of the potential around the particular scale ϕ_0 (in our case, ϕ_0 is the inflaton value at the epoch of horizon exit for the pivot scale $k_0 \approx 0.002h \text{ Mpc}^{-1}$) is

$$V(\phi) = V_0 + \frac{\phi^2}{2} \left[m^2(\ln(\phi_0)) - c \frac{V_0}{M_P^2} \ln \frac{\phi}{\phi_0} + \dots \right]. \quad (24)$$

Here, constant c is defined by the equation

$$c \frac{V_0}{M_P^2} = - \left. \frac{dm^2}{d \ln \phi} \right|_{\phi=\phi_0}. \quad (25)$$

In turn, a Taylor expansion of eq. (22) up to linear terms gives ($t_0 = \ln \frac{\phi_0}{M_P}$):

$$m^2(t) = m^2(t_0) - 4\tilde{m}_0^2 \frac{\tilde{\alpha}_0}{(1 + \tilde{\alpha}_0 t_0)^3} \ln \frac{\phi}{\phi_0}. \quad (26)$$

From eqs. (25) and (26) we obtain the expression for the constant c ,

$$c \frac{V_0}{M_P^2} = 4\tilde{m}_0^2 \frac{\tilde{\alpha}_0}{(1 + \tilde{\alpha}_0 t_0)^3}. \quad (27)$$

If $|m_0^2| \sim \tilde{m}_0^2 \approx H_I^2$, then

$$c = \frac{4}{3} \frac{\tilde{\alpha}_0}{(1 + \tilde{\alpha}_0 t_0)^3}. \quad (28)$$

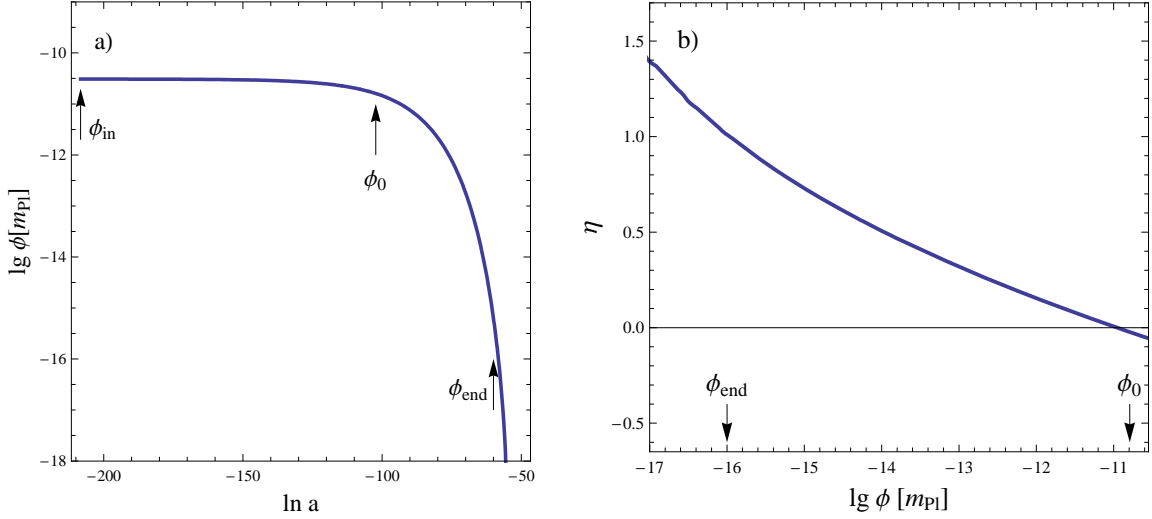


Figure 7: **a)** Evolution of the inflaton field $\phi(\ln a)$ in the running mass model. **b)** The dependence of the parameter η on a value of the field ϕ . For both plots, $H_I = 10^{-15} M_P$, $c = 0.062$, $s = 0.040$.

It appears (see fig. 7b) that in our example $\phi_0 \sim 10^{-10} M_P$, so $t_0 \sim \ln 10^{-10} \sim (-23)$. Assuming that $\alpha_0 \sim 1/24$ (as in SUSY-GUT models), one has $\tilde{\alpha}_0 \sim \frac{2}{2\pi} \frac{1}{24}$. In such a case, $c \sim 4\tilde{\alpha}_0 \sim 0.06$.

If we would keep terms of higher order in $t - t_0 = \ln \frac{\phi}{\phi_0}$ in the Taylor expansion of $m^2(t)$ in eq. (26) we would see that the real expansion parameter is $\tilde{\alpha}_0 \ln \frac{\phi}{\phi_0}$ rather than $\ln \frac{\phi}{\phi_0}$. The smallest value of ϕ , ϕ_{end} , in our case is $\sim 10^{-16} M_P$ (see fig. 7b). Even for such value of ϕ_{end} , the expansion parameter is rather small,

$$\tilde{\alpha}_0 \ln \frac{\phi_{\text{end}}}{\phi_0} \sim \tilde{\alpha}_0 \ln 10^{-6} \sim (-0.1) . \quad (29)$$

Having this in mind, we will use the linear approximation for the inflaton mass (eq. (26)) in the entire region of inflaton field values exploited in the present paper.

Following the previous papers, we introduce another parameter,

$$s = c \ln \left(\frac{\phi_*}{\phi_0} \right) , \quad (30)$$

where ϕ_* is the inflaton value corresponding to the maximum of the potential. This parameter connects the field value ϕ_0 with the Hubble parameter during inflation and with the normalization of the CMB power spectrum:

$$\phi_0 s = \frac{H_I}{2\pi \mathcal{P}_{\mathcal{R}}^{1/2}(k_0)} . \quad (31)$$

4. The minimum value of the inflaton field which corresponds to the end of inflation can be determined from the approximate equation [28]

$$\eta = M_P^2 \frac{V''}{V} \cong \frac{M_P^2}{V_0} m^2 = 1 . \quad (32)$$

Using RGE, one obtains from this formula the relation

$$\frac{M_P^2}{V_0} \left(m_0^2 - A\tilde{m}_0^2 + \frac{A\tilde{m}_0^2}{(1 + \tilde{\alpha}_0 t)^2} \right) = 1 . \quad (33)$$

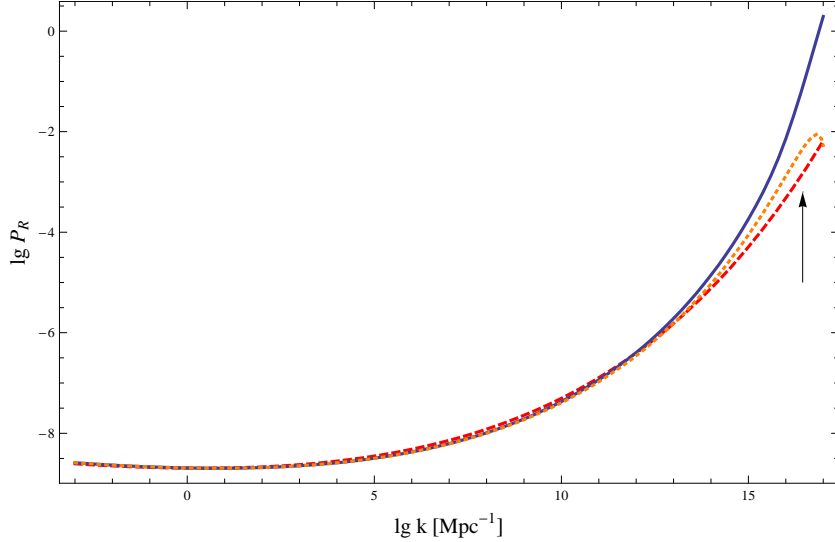


Figure 8: Power spectrum $\mathcal{P}_{\mathcal{R}}(k)$ in the running mass model, calculated numerically (solid line), by the approximate analytic formula (39) (long-dashed line) and using the Stewart-Lyth extended slow-roll approximation (short-dashed line). The parameters of the potential are the same as used in fig. 7. The arrow shows the value of k_{end} .

Substituting here $A = 2$, $\tilde{m}_0^2 = |m_0^2| = V_0/3M_P^2$, one has finally the approximate expression for ϕ_{end} ,

$$\phi_{\text{end}} = M_P e^{-\frac{1}{\tilde{\alpha}_0} \left(1 - \frac{1}{\sqrt{3}}\right)}, \quad (34)$$

which shows that the minimum field value is very sensitive to the value of the model parameter $\tilde{\alpha}_0$ and, in our case, does not depend on V_0 . More exactly, the condition $\eta = 1$ means the end of the slow-roll part of inflation. We suppose, as usual (see, e.g. [24, 25]) that in reality inflation ends by hybrid mechanism, and the critical value of inflaton field, ϕ_{cr} , is determined by the value of the Yukawa coupling λ (in spite of the inequality $\lambda^2 \ll \alpha$). One can check [28] that the value of λ can always be chosen such that $\phi_{\text{cr}} < \phi_{\text{end}}$ and slow-roll ends before the reaching of ϕ_{cr} .

One should note that the accuracy of the approximate formula (34) is not very good. Luckily, in the approach based on the numerical calculation of the power spectrum there is no need to use it, because the value of ϕ_{end} appears in a course of the calculation (fig. 7b).

3.2 Power spectrum of curvature perturbations

An analysis of CMB anisotropy data [31, 32], including other types of observation [33], leads to the following main qualitative conclusions:

i) the power spectrum of scalar curvature perturbations is red, i.e., the spectral index is negative,

$$n_0 = 0.97 \pm 0.01 ; \quad (35)$$

ii) observations are consistent, or, at least, are not in contradiction with the small positive running of the spectral index, $n'_0 < 0.01$;

iii) the contribution of tensor perturbations in the value of the spectral index is small ($\lesssim 10^{-2}$) and, as a result, $n \approx 1 + 2\eta$; it means that η is negative, and the potential must be concave-downward (i.e., of hill-top type), while cosmological scales cross horizon during inflation [1].

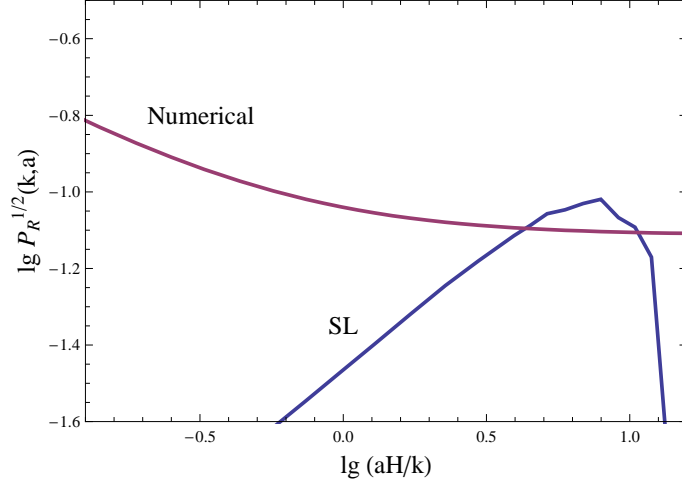


Figure 9: Dependence of $\mathcal{P}_{\mathcal{R}}(k, a)$ calculated numerically and $\mathcal{P}_{\mathcal{R}}$ from the Stewart-Lyth formula. The comoving wave number for this figure is $k = 10^{15.8} \text{ Mpc}^{-1}$.

These conclusions constrain the possible values of the parameters s and c . Approximately, for cosmological scale one has

$$n_0 - 1 \approx 2(s - c) \quad , \quad n'_0 \approx 2sc \quad . \quad (36)$$

From *iii*) follows that $c > 0$ (it is consistent with eq. (31)), from the positivity of n'_0 (conclusion *ii*)) follows that $s > 0$. At last, *i*) leads to inequality $s < c$.

We choose for the power spectrum calculation the following values:

$$c = 0.062 \quad , \quad s = 0.040. \quad (37)$$

These numbers correspond, at cosmological scales, to the following values of slow-roll parameters:

$$\epsilon \approx \frac{s\phi_0^2}{M_P^2} \sim 10^{-21} \quad ; \quad \eta \approx s - c \sim (-0.02) \quad , \quad (38)$$

that seems to be consistent with the present data [4].

To check the validity of the slow-roll approximation, we calculate the spectrum by three ways: *i*) using the approximate analytic slow-roll formula

$$\mathcal{P}_{\mathcal{R}}(k) = \mathcal{P}_{\mathcal{R}}(k_0) \exp \left[\frac{2s}{c} \left(e^{c\Delta N(k)} - 1 \right) - 2c\Delta N(k) \right] \quad ; \quad \Delta N(k) = \ln \frac{k}{k_0} \quad (39)$$

(this expression is easily derived from the simplest slow-roll prediction (2)); *ii*) using the Stewart-Lyth approximation (3); *iii*) by numerical integration of the differential equation for \mathcal{R}_k (7).

The results of the calculations are presented in figs. 7-9. Fig. 7 shows the evolution of the inflaton field ϕ with scale factor and a growth of the slow-roll parameter η with a decrease of ϕ from ϕ_0 to ϕ_{end} . The power spectrum is shown in fig. 8 for a broad interval of comoving wave numbers. It is clearly seen that near the end of inflation, when

$$\phi \sim 10^{-16} M_P \quad , \quad k \sim k_{\text{end}} = a_{\text{end}} H_{\text{end}} = 3 \times 10^{16} \text{ Mpc}^{-1} \quad , \quad (40)$$

the slow-roll formulae are inaccurate: they strongly underestimate values of $\mathcal{P}_{\mathcal{R}}$. To illustrate this point more clearly, at the next figure we show the comparison of two curves: aH -dependence of the spectrum calculated numerically for a definite value of k , $k = 10^{15.8} \text{ Mpc}^{-1}$, and aH -dependence of the Stewart-Lyth spectrum. It is seen that the numerical spectrum at the moment of crossing horizon (when $aH = k$) is already almost asymptotical, and its value distinctly exceeds the corresponding value predicted by Stewart-Lyth formula.

3.3 Quantum diffusion effects

We calculate the curvature perturbations in terms of the classical trajectories of a scalar field associating, in particular, points in field space with definite numbers of e-folds from the end of inflation. This description becomes incorrect if the quantum diffusion destroys the classical evolution of the field. In this case we should use the methods of stochastic inflation. This approach operates with the coarse-grained field, which is defined to be spatial average of the field ϕ over a physical volume with size larger than the Hubble radius H^{-1} .

In the slow-roll approximation, the evolution of the coarse-grained field φ is governed by the first order Langevin-like equation [34, 35, 36]

$$\dot{\varphi} + \frac{1}{3H}V'(\varphi) = \frac{H^{3/2}}{2\pi}\xi(t), \quad (41)$$

$$\langle \xi(t) \rangle = 0, \quad \langle \xi(t)\xi(t') \rangle = \delta(t - t'). \quad (42)$$

Here, $\xi(t)$ is a random noise field, and angular brackets mean ensemble average. The term $\frac{1}{3H}V'(\varphi)$ describes the deterministic evolution of the field φ , in the absence of the noise term $\frac{H^{3/2}}{2\pi}\xi(t)$. The solution of eq. (41), in the absence of the noise term, is the deterministic slow-roll trajectory $\varphi_{\text{sr}}(t)$. Going to finite time differences, the coefficient $\frac{H^{3/2}}{2\pi}$ can be rewritten as $\sqrt{\frac{H^3}{4\pi^2\Delta t}}$, and the evolution of φ on the timescales $\Delta t \geq H^{-1}$ can be described by a finite-difference form of the eq. (41),

$$\varphi(t + \Delta t) - \varphi(t) = -\frac{1}{3H}V'(\varphi)\Delta t + \frac{1}{2\pi}\sqrt{H^3\Delta t}\xi(t). \quad (43)$$

The condition for the deterministic evolution is (see e.g. [37])

$$\frac{1}{3H}|V'(\varphi)|\Delta t \gg \frac{1}{2\pi}\sqrt{H^3\Delta t}, \quad \Delta t = H^{-1}. \quad (44)$$

Using the slow-roll connection between V and H , one obtains

$$|V'(\varphi)| \gg \frac{3}{2\pi}H^3 = \frac{1}{2\pi\sqrt{3}}V^{3/2}(\varphi). \quad (45)$$

In the approach of [38] the coarse-grained field is considered as a perturbation of the classical solution φ_{cl} (that is, the solution of the Langevin equation without the noise),

$$\varphi(t) = \varphi_{\text{cl}}(t) + \delta\varphi_1(t) + \delta\varphi_2(t) + \dots. \quad (46)$$

Here, the term $\delta\varphi_i(t)$ depends on the noise at the power i . It is assumed that the Hubble parameter in the Langevin equation depends only on the coarse-grained field φ ,

$$H^2(\varphi) = \frac{1}{3M_P^2}V(\varphi). \quad (47)$$

Correspondingly, the Hubble parameter can be expanded perturbatively,

$$H(\varphi) = H_{\text{cl}} + H'_{\text{cl}}(\delta\varphi_1 + \delta\varphi_2) + \frac{H''_{\text{cl}}}{2}\delta\varphi_1^2 + \dots, \quad (48)$$

$$H_{\text{cl}} = H(\varphi_{\text{cl}}) = \sqrt{\frac{V(\varphi_{\text{cl}})}{3M_P^2}}. \quad (49)$$

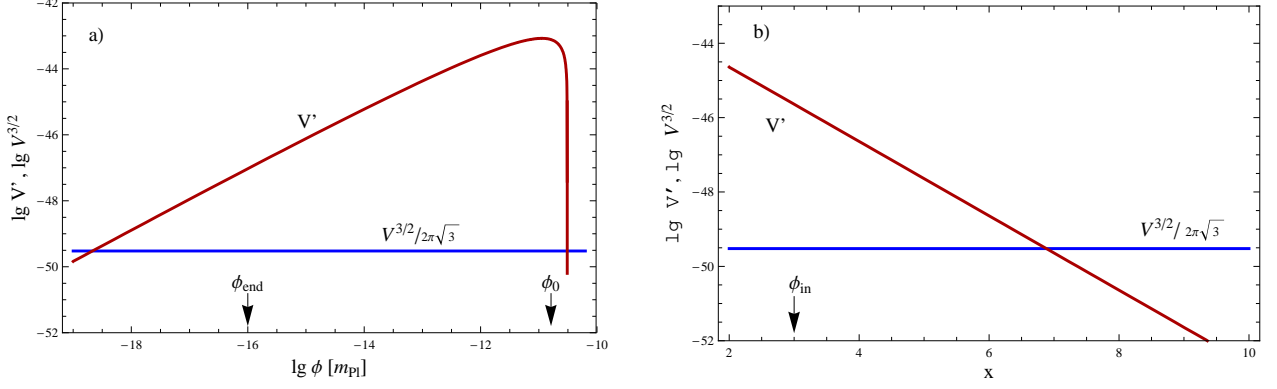


Figure 10: **a)** Comparison of V' and $V^{3/2}$ for the running mass model (see eq. (45)). **b)** The same figure in different scale: variable x is connected to the field value by the relation $\varphi = (1 - 10^{-x})\varphi_*$.

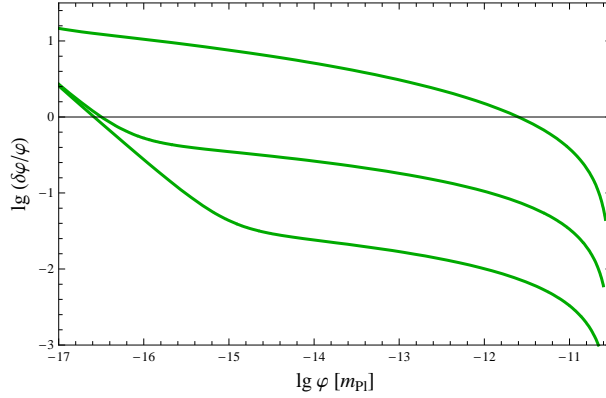


Figure 11: The result for the calculation of $\delta\varphi/\varphi$ for different values of $\varphi_{\text{in}} = \varphi_*(1 - 10^{-x})$. From bottom to top, x equals 3, 4, 5. Here, $\delta\varphi \equiv \sqrt{\langle\delta\varphi_1^2\rangle + \langle\delta\varphi_2^2\rangle}$.

This approach permits to calculate the mean value of the total number of e-folds, $\langle N \rangle$, and to compare it with the corresponding "classical" number,

$$N_T^{\text{cl}} = -\frac{1}{2M_P^2} \int_{\varphi_{\text{in}}}^{\varphi_{\text{end}}} d\varphi_{\text{cl}} \frac{H_{\text{cl}}}{H'_{\text{cl}}} = \frac{1}{M_P^2} \int_{\varphi_{\text{end}}}^{\varphi_{\text{in}}} d\varphi_{\text{cl}} \left(\frac{V}{V'} \right), \quad (50)$$

$$\delta N_T = \langle N_T \rangle - N_T^{\text{cl}} = -\frac{1}{2M_P^2} \int_{\varphi_{\text{in}}}^{\varphi_{\text{end}}} \left[\langle \delta\varphi_2 \rangle + \frac{H''_{\text{cl}}}{2H'_{\text{cl}}} \langle \delta\varphi_1^2 \rangle \right] d\varphi_{\text{cl}}. \quad (51)$$

Besides, one can calculate the mean value of the Gaussian probability distribution function for the coarse-grained field and to see how it behaves as a function of the current field value.

The interval of inflaton field values for which the inequality (45) holds and, therefore, the deterministic evolution dominates, is shown in fig. 10a,b. The variable x in fig. 10b is defined by the relation

$$\frac{\varphi_{\text{in}}}{\varphi_*} = 1 - 10^{-x} \quad (52)$$

(φ_* is, as before, the point of a maximum of the potential $V(\varphi)$). It is seen from the figure that the constraints on the inflaton field following from condition (45) are not too severe,

$$3 \times 10^{-19} M_P \lesssim \varphi \lesssim \varphi_* - 10^{-7} \varphi_*. \quad (53)$$

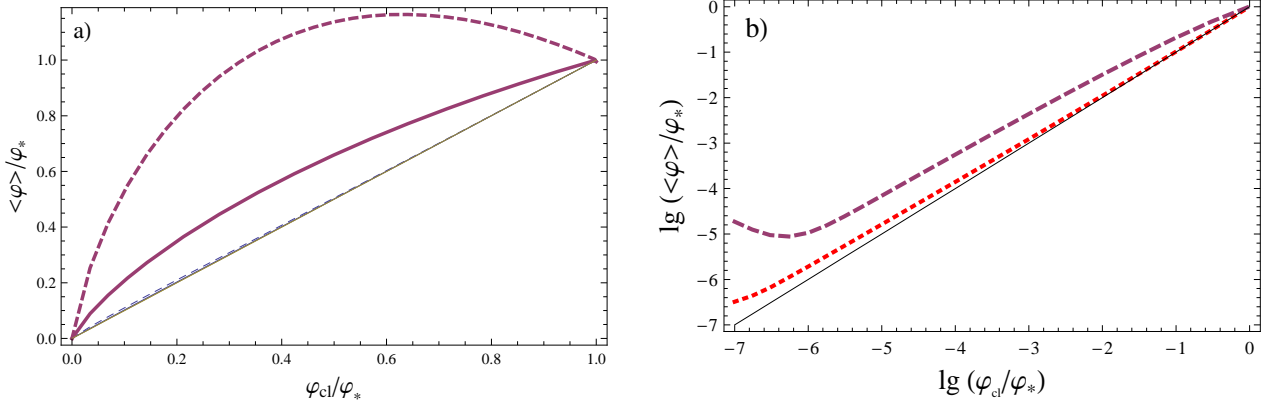


Figure 12: Calculation of stochastic effects for various values of initial field φ_{in} . **a)** Thin dashed curve: $\varphi_{in} = (1 - 1.5 \times 10^{-5})\varphi_*$, no volume effects included; thick dashed curve: $\varphi_{in} = (1 - 1.5 \times 10^{-5})\varphi_*$, volume effects included; solid thick curve: $\varphi_{in} = (1 - 3 \times 10^{-5})\varphi_*$, volume effects included. **b)** Thick long-dashed and thick short-dashed curves correspond to the cases with and without inclusion of volume effects, respectively, for $\varphi_{in} = (1 - 3 \times 10^{-5})\varphi_*$.

An accuracy of the perturbative expansion (46) for the potential of stochastic inflation models was studied in [39]. Here we study this accuracy for the running mass potential, using the parameters V_0 , s , c , φ_{end} introduced above. The results of the calculation of $\langle \delta\varphi_1^2 \rangle$ and $\langle \delta\varphi_2 \rangle$ are shown in fig. 11. As one can see, the perturbative expansion is good if the starting value of the inflaton field, φ_{in} , is chosen to be not too close to the value of φ at the maximum of the potential. More exactly, the parameter x , defined in (52), must be smaller than $4 \div 4.5$. Starting value φ_{in} corresponds to the beginning of the evolution, i.e., $\delta\varphi_1(t_{in}) = \delta\varphi_2(t_{in}) = 0$.

If the evolution is deterministic, the correction to a classical e-fold number N_T^{cl} , given by eq. (51), is small. To estimate analytically the upper limit for this correction, we used the analytic expressions for $\langle \delta\varphi_1^2 \rangle$ and $\langle \delta\varphi_2 \rangle$ derived in [38], keeping in them leading terms only. According to these expressions, the following inequalities hold:

$$\langle \delta\varphi_2 \rangle < \left(\frac{V_0}{M_P} \right)^4 \left(\frac{M_P}{\varphi_{in}} \right)^2 \frac{1}{\ln^2 \frac{\varphi_{in}}{\varphi_*}} \frac{\varphi}{M_P} \lesssim 10^{-10+2x} \varphi, \quad (54)$$

$$\langle \delta\varphi_1^2 \rangle < \left(\frac{V_0}{M_P} \right)^4 \frac{1}{\ln^2 \frac{\varphi_{in}}{\varphi_*}} \sim 10^{-30+2x} M_P^2. \quad (55)$$

Using these upper limits, one can estimate the corresponding upper limits of two integrals in the expression for δN_T (51). The result is the following:

$$\frac{1}{M_P^2} \int_{\varphi_{end}}^{\varphi_{in}} \langle \delta\varphi_2 \rangle d\varphi_{cl} < 10^{-30+2x}; \quad \frac{1}{M_P^2} \int_{\varphi_{end}}^{\varphi_{in}} \frac{\langle \delta\varphi_1^2 \rangle H_{cl}''}{H_{cl}'} d\varphi_{cl} < 10^{-30+3x}. \quad (56)$$

It is clear from eq. (56) that the quantum correction to e-fold number, δN_T , is quantitatively small even if the value of x is as large as 10. But only if $x < 4 \div 4.5$, and the perturbative expression is valid one really can be sure that

$$\delta N_T \ll N_T^{cl}, \quad (57)$$

and the evolution is deterministic.

However, this analysis is still not complete: one must check also the position of the mean value of the probability distribution function for the coarse-grained field [38]. The calculation,

with taking into account the volume effects, leads to the results shown in fig. 12a,b. It is seen from the figure that in this case also, as in the calculation of the e-fold number correction, the correct choice of the initial condition plays a decisive role: there are no effects of a "walk" of the mean value around the maximum of the potential (such effects were noticed in [38]) if evolution starts from the point which is far enough from the maximum ($x \lesssim 4.5$). Of course, the realization of the initial condition of this kind is, in itself, a problem. Supposedly, it could be provided by the previous history of eternal inflation [24, 25].

4 Conclusions

1. It is shown, by numerical methods, that in the single-field inflationary model with a simple double-well potential the parameter values of this potential can be chosen in such a way that the power spectrum of curvature perturbations $\mathcal{P}_{\mathcal{R}}(k)$ has a huge peak (with amplitude ~ 0.1) at large k (and the right normalization and monotonic behavior at cosmological scales). The peak arises due to temporary interruption of the slow-roll near points of the minimum of the potential, $\pm v$. The corresponding mass of PBHs produced in early universe in a case of the realization of such power spectrum is about $10^7 g$.

The analogous behavior of the power spectrum was obtained by authors of [3] in a model with CW potential. There are some important differences in the results of [3] and ours, in the peak amplitude and PBH mass, connected, in particular, with a large flatness near the origin in a case of the CW potential.

2. It is shown that the inflation model with running mass potential predicts a rather large amplitude of the power spectrum of curvature perturbations (~ 0.1) at k -values $\sim 10^{16} \text{ Mpc}^{-1}$. For such a prediction, a very small positive spectral index running at cosmological scales is necessary, $n' \sim 0.005$, as well as a small negative value for the slow-roll parameter η (≈ -0.02). Both this numbers do not contradict with data. It is shown also that for an obtaining the correct quantitative results for the power spectrum at largest k -values an use of numerical methods is required because, in general, slow-roll formulas are not accurate enough at the end of inflation, where $\eta \approx 1$.

3. Quantum diffusion effects in the model with running mass potential are studied in details. It is shown that inflationary evolution of the universe in a model with a scalar field and running mass potential can be described by the classic deterministic equations, and for a possibility of such a description the correct choice of the initial conditions is crucial. Concretely, an initial value of the inflaton field (at the beginning of the evolution) should not be too close to a point of the maximum of the potential. If this condition is satisfied, the quantum corrections to a total e-fold number and to a position of the mean value of the probability distribution function are small.

Acknowledgements. The work was supported by Russian Foundation for Basic Research (grant 06-02-16135).

References

- [1] K. Kohri, C. M. Lin and D. H. Lyth, JCAP **0712**, 004 (2007) [arXiv:0707.3826 [hep-ph]].
- [2] K. Kohri, D. H. Lyth and A. Melchiorri, JCAP **0804**, 038 (2008) [arXiv:0711.5006 [hep-ph]].
- [3] R. Saito, J. Yokoyama and R. Nagata, arXiv:0804.3470 [astro-ph].
- [4] H. V. Peiris and R. Easther, arXiv:0805.2154 [astro-ph].
- [5] L. Boubekeur and D. H. Lyth, JCAP **0507**, 010 (2005) [arXiv:hep-ph/0502047].
- [6] J. Yokoyama, Phys. Rev. D **58**, 083510 (1998) [arXiv:astro-ph/9802357].

- [7] S. M. Leach, I. J. Grivell and A. R. Liddle, Phys. Rev. D **62**, 043516 (2000) [arXiv:astro-ph/0004296].
- [8] V. N. Lukash, JETP Lett. **31** (1980) 596; Sov. Phys. JETP **52** (1980) 807.
- [9] V. F. Mukhanov, JETP Lett. **41**, 493 (1985); Sov. Phys. JETP **67**, 1297 (1988).
- [10] M. Sasaki, Prog. Theor. Phys. **76**, 1036 (1986).
- [11] V. F. Mukhanov, H. A. Feldman and R. H. Brandenberger, Phys. Rept. **215**, 203 (1992).
- [12] A. R. Liddle and D. H. Lyth, Phys. Rept. **231**, 1 (1993) [arXiv:astro-ph/9303019].
- [13] E. D. Stewart and D. H. Lyth, Phys. Lett. B **302**, 171 (1993) [arXiv:gr-qc/9302019].
- [14] J. O. Gong and E. D. Stewart, Phys. Lett. B **510**, 1 (2001) [arXiv:astro-ph/0101225].
- [15] P. Ivanov, P. Naselsky and I. Novikov, Phys. Rev. D **50** (1994) 7173.
- [16] J. S. Bullock and J. R. Primack, Phys. Rev. D **55** (1997) 7423 [arXiv:astro-ph/9611106].
- [17] S. M. Leach and A. R. Liddle, Phys. Rev. D **63**, 043508 (2001) [arXiv:astro-ph/0010082].
- [18] S. M. Leach, M. Sasaki, D. Wands and A. R. Liddle, Phys. Rev. D **64**, 023512 (2001) [arXiv:astro-ph/0101406].
- [19] S. R. Coleman and E. Weinberg, Phys. Rev. D **7**, 1888 (1973).
- [20] Ya. B. Zeldovich, I. D. Novikov, Sov. Astron. A.J. **10** (1967) 602.
- [21] S. Hawking, Mon. Not. Roy. Astron. Soc. **152** (1971) 75.
- [22] B. J. Carr, “*Primordial Black Holes: Do They Exist and Are They Useful?*”, arXiv:astro-ph/0511743.
- [23] M. Y. Khlopov, arXiv:0801.0116 [astro-ph].
- [24] E. D. Stewart, Phys. Lett. B **391**, 34 (1997) [arXiv:hep-ph/9606241].
- [25] E. D. Stewart, Phys. Rev. D **56**, 2019 (1997) [arXiv:hep-ph/9703232].
- [26] L. Covi and D. H. Lyth, Phys. Rev. D **59**, 063515 (1999) [arXiv:hep-ph/9809562].
- [27] L. Covi, D. H. Lyth and L. Roszkowski, Phys. Rev. D **60**, 023509 (1999) [arXiv:hep-ph/9809310].
- [28] L. Covi, Phys. Rev. D **60**, 023513 (1999) [arXiv:hep-ph/9812232].
- [29] G. German, G. G. Ross and S. Sarkar, Phys. Lett. B **469**, 46 (1999) [arXiv:hep-ph/9908380].
- [30] L. Covi, D. H. Lyth, A. Melchiorri and C. J. Odman, Phys. Rev. D **70**, 123521 (2004) [arXiv:astro-ph/0408129].
- [31] D. N. Spergel *et al.* [WMAP Collaboration], Astrophys. J. Suppl. **170**, 377 (2007) [arXiv:astro-ph/0603449].
- [32] J. Dunkley *et al.* [WMAP Collaboration], arXiv:0803.0586 [astro-ph].
- [33] J. Lesgourgues, M. Viel, M. G. Haehnelt and R. Massey, JCAP **0711**, 008 (2007) [arXiv:0705.0533 [astro-ph]].
- [34] A. Vilenkin, Phys. Rev. D **27**, 2848 (1983); Nucl. Phys. B **226**, 527 (1983).
- [35] J. M. Bardeen, P. J. Steinhardt and M. S. Turner, Phys. Rev. D **28**, 679 (1983).
- [36] A. D. Linde, Phys. Lett. B **175**, 395 (1986).
- [37] S. Winitzki, Lect. Notes Phys. **738** (2008) 157 [arXiv:gr-qc/0612164].
- [38] J. Martin and M. Musso, Phys. Rev. D **73** (2006) 043516 [arXiv:hep-th/0511214].
- [39] J. Martin and M. Musso, Phys. Rev. D **73** (2006) 043517 [arXiv:hep-th/0511292].